HHS Public Access

Author manuscript

J Cell Physiol. Author manuscript; available in PMC 2015 December 30.

Published in final edited form as:

J Cell Physiol. 2011 November ; 226(11): 2925–2933. doi:10.1002/jcp.22640.

Hypoxia-Inducible Factor 1 Mediates Increased Expression of NADPH Oxidase-2 in Response to Intermittent Hypoxia

Guoxiang Yuan[1], **Shakil A. Khan**[1], **Weibo Luo**[2,3,4], **Jayasri Nanduri**[1], **Gregg L. Semenza**[2,3,4], and **Nanduri R. Prabhakar**[1,*]

[1]Institute for Integrative Physiology and The Center for Systems Biology of O2 Sensing, Biological Science Division, University of Chicago, Illinois [2]Vascular Program, Institute for Cell Engineering, The Johns Hopkins University School of Medicine, Baltimore, Maryland [3]Department of Pediatrics, Medicine, Oncology, Radiation Oncology, and Biological Chemistry, The Johns Hopkins University School of Medicine, Baltimore, Maryland [4]McKusick-Nathans Institute of Genetic Medicine, The Johns Hopkins University School of Medicine, Baltimore, Maryland

Abstract

Sleep-disordered breathing with recurrent apnea is associated with intermittent hypoxia (IH). Cardiovascular morbidities caused by IH are triggered by increased generation of reactive oxygen species (ROS) by pro-oxidant enzymes, especially NADPH oxidase-2 (Nox2). Previous studies showed that (i) IH activates hypoxia-inducible factor 1 (HIF-1) in a ROS-dependent manner and (ii) HIF-1 is required for IH-induced ROS generation, indicating the existence of a feed-forward mechanism. In the present study, using multiple pharmacological and genetic approaches, we investigated whether IH-induced expression of Nox2 is mediated by HIF-1 in the central and peripheral nervous system of mice as well as in cultured cells. IH increased Nox2 mRNA, protein, and enzyme activity in PC12 pheochromocytoma cells as well as in wild-type mouse embryonic fibroblasts (MEFs). This effect was abolished or attenuated by blocking HIF-1 activity through RNA interference or pharmacologic inhibition (digoxin or YC-1) or by genetic knockout of HIF-1α in MEFs. Increasing HIF-1α expression by treating PC 12 cells with the iron chelator deferoxamine for 20 h or by transfecting them with HIF-1alpha expression vector increased Nox2 expression and enzyme activity. Exposure of wild-type mice to IH (8 h/day for 10 days) up-regulated Nox2 mRNA expression in brain cortex, brain stem, and carotid body but not in cerebellum. IH did not induce Nox2 expression in cortex, brainstem, carotid body, or cerebellum of *Hif1a*$^{+/-}$ mice, which do not manifest increased ROS or cardiovascular morbidities in response to IH. These results establish a pathogenic mechanism linking HIF-1, ROS generation, and cardiovascular pathology in response to IH.

Sleep disordered breathing with recurrent apnea (transient, repetitive cessation of breathing) is a major cause of morbidity and mortality in adult humans (Nieto et al., 2000) and pre-term infants (Poets et al., 1994). Recurrent apneas are associated with periodic decreases in arterial blood oxygen or intermittent hypoxia (IH). Humans with recurrent apnea and rodents

*Correspondence to: Nanduri R. Prabhakar, Institute for Integrative Physiology & The Center for Systems Biology of O_2 Sensing, Department of Medicine, MC 5068, 5841 South Maryland, Avenue, Chicago, IL 60637. nanduri@uchicago.edu.

exposed to IH exhibit autonomic morbidities including persistent sympathetic activation, hypertension, and elevated circulating catecholamines (Narkiewicz and Somers, 1997; Peppard et al., 2000; Prabhakar and Kumar, 2010). Studies on humans (Narkiewicz and Somers, 1997) and rodent models of IH (Fletcher et al., 1992; Peng et al., 2006) have shown that the carotid body, which is the primary chemoreceptor for detecting changes in arterial PO_2, responds to IH by triggering reflex activation of the sympathetic nervous system and enhanced catecholamine secretion from adrenal medullary chromaffin cells (AMC), leading to elevated circulating catecholamines and elevated blood pressure (Bao et al., 1997; Kumar et al., 2006; Souvannakitti et al., 2009). IH increases the levels of reactive oxygen species (ROS) in the carotid body (Peng et al., 2003) and adrenal medulla (Kumar et al., 2006; Souvannakitti et al., 2009). Anti-oxidant treatment prevents increased carotid body function (Peng et al., 2003; Peng and Prabhakar, 2004; Del Rio et al., 2010), augmented catecholamine secretion from AMC (Kumar et al., 2006; Kuri et al., 2007; Souvannakitti et al., 2009), and elevated blood pressure (Peng et al., 2006; Troncoso Brindeiro et al., 2007), indicating that ROS signaling is a critical cellular mechanism underlying IH-evoked autonomic morbidities.

NADPH oxidase (Nox) activity is a major source of cellular ROS (Bedard and Krause, 2007). IH leads to increased expression of several Nox isoforms in the carotid body (Peng et al., 2009), AMC (Souvannakitti et al., 2010), and central nervous system (CNS; Zhan et al., 2005) as well as in cultured PC12 rat pheochromocytoma cells, which are derived from AMC (Yuan et al., 2008). Of the various Nox isoforms, Nox2 has been implicated in mediating the effects of IH on carotid body function (Peng et al., 2009), catecholamine secretion from AMC (Souvannakitti et al., 2010), and sleep behavior (Zhan et al., 2005). However, mechanisms underlying increased *Nox2* gene expression in response to IH have not been elucidated.

The transcriptional activator hypoxia-inducible factor 1 (HIF-1) is a master regulator of O_2 homeostasis that controls multiple physiological processes by regulating the expression of hundreds of genes (Mole et al., 2009; Semenza, 2009). HIF-1 is a heterodimeric protein composed of a constitutively expressed HIF-1β subunit and an O_2-regulated HIF-1α subunit (Wang et al., 1995). We previously reported that IH increases HIF-1α protein levels in PC12 cell cultures (Yuan et al., 2005, 2008) and in mice (Peng et al., 2006). In catecholamine-producing PC12 cells, the induction of HIF-1α protein levels by IH requires ROS-dependent activation of phospholipase Cγ (PLCγ), protein kinase C (PKC), and mammalian target of rapamycin (mTOR; Yuan et al., 2008). Physiological studies of wild-type (WT) mice exposed to IH revealed striking autonomic morbidities, including heightened carotid body activity, elevated plasma catecholamines, exaggerated hypoxic ventilatory response, and hypertension (Peng et al., 2006). In contrast, littermate *Hif1a*$^{+/-}$ mice, which are heterozygous for a null [knockout (KO)] allele at the locus encoding HIF-1α, do not display any of these IH-induced autonomic responses (Peng et al., 2006). Furthermore, ROS levels were significantly increased in the CNS of IH-exposed WT mice, but not in *Hif1a*$^{+/-}$ mice (Peng et al., 2006). Taken together, these results indicated that IH-induced ROS leads to HIF-1 activation, which leads to further ROS generation, thereby creating a feed-forward mechanism that is essential for the pathogenesis of cardiovascular and respiratory

abnormalities. Establishing the molecular mechanism by which HIF-1 increases ROS generation is the critical next step in understanding the pathobiology of IH. Based on the observations described above, we tested the hypothesis that in response to IH, HIF-1 increases ROS generation by activation of the *Nox2* gene.

Materials and Methods

Cell culture

PC12 cells (original clone from Dr. L. Green) were cultured in Dulbecco's modified Eagle's medium (DMEM) supplemented with 10% horse serum, 5% fetal bovine serum (FBS), penicillin (100 U/ml), and streptomycin (100 μg/ml) under 90% air and 10% CO_2 at 37°C. Prior to all experiments, the cells were placed in antibioticfree medium and serum starved for 16 h to avoid any confounding effects of serum on HIF-1 activity. In the experiments involving treatment with drugs, cells were pre-treated for 30 min with either drug or vehicle. Immortalized fibroblasts were derived from WT and *Hif1a*$^{-/-}$ mouse embryos as previously reported (Feldser et al., 1999).

Exposure of cells to IH

Cell cultures were exposed to IH as described previously (Yuan et al., 2005). Cells were exposed to alternating cycles of 1.5% O_2 for 30 sec followed by 20% O_2 for 5 min at 37°C. Gas flows were controlled by timer-controlled solenoid valves. O_2 levels were monitored by an electrode (Lazar Research Laboratories Inc, Los Angeles, CA) placed in the tissue culture medium and ambient O_2 levels were monitored by an O_2 analyzer (Alpha Omega Instruments, Cumberland, RI).

Exposure of mice to IH

Experiments involving mice were approved by the Institutional Animal Care and Use Committee of the University of Chicago and were performed on age- and gender-matched WT (Hif1a$^{+/+}$) and Hif1a$^{+/-}$ mice (Iyer et al., 1998). Unrestrained, freely moving mice (body weight, 20–25 g) housed in feeding cages were exposed to IH for 8 h per day for 10 days as previously described (Peng et al., 2006). Briefly, mice were placed in a specialized chamber, which was flushed with alternating cycles of pure nitrogen and compressed air. During hypoxia, inspired O_2 levels rapidly reached a nadir of 5% O_2. The gas flows were regulated by timer-controlled solenoid valves. Ambient O_2 and CO_2 levels in the chamber were continuously monitored by an O_2/CO_2 analyzer (Alpha Omega Instrument, Cumberland, RI; Series 9500). Control experiments were performed on animals exposed to alternating cycles of compressed room air instead of hypoxia in the same chamber.

Chemicals

All chemicals and reagents were of analytical grade and obtained from Sigma Chemical Co. (St. Louis, MO) unless otherwise stated.

Immunoblot assays

Immunoblot assays were performed as described previously (Yuan et al., 2005). Briefly, cell extracts (25 μg) were fractionated by 7.5% PAGE–SDS gel electrophoresis and transferred to a polyvinylpyrrolidone difluoride membrane (Immobilon-P, Millipore, Bedford, MA). The membrane was blocked with Tris-buffered saline (TBS-T) containing 5% non-fat milk and incubated with anti-HIF-1α monoclonal antibody (Novus Biologicalsm, Littleton, CO) at 1:500 dilution in blocking buffer. Membranes were treated with goat anti-rabbit secondary antibody conjugated with horseradish peroxidase (Chemicon, Temecula, CA; 1:2,000 dilution) and immune complexes were visualized using enhanced chemiluminescence detection system (Amersham BioSciences, Piscataway, NJ). Similar procedures were employed for immunoblot analysis of Nox2 (Santa Cruz, Santa Cruz, CA, dilution 1:2,000), α-tubulin (Sigma, St. Louis, MO; 1:3,000), PLCγ1 (Cell Signaling, Danvers, MA; 1:1,000), phosphorylated PLCγ1 (Cell Signaling; 1:2,000), mTOR (Cell Signaling; 1:1,000), phosphorylated mTOR (Cell Signaling; 1:1,000), and phosphorylated PKC (anti-pan $PKC\gamma^{Thr514}$; Cell Signaling; 1:1,000).

Transient transfection and reporter gene assay

To analyze HIF-1 transcriptional activity, cells were co-transfected with two reporter plasmids: p2.1, which contains firefly luciferase coding sequences downstream of a basal SV40 promoter and a 68 bp hypoxia response element (HRE) from the human *ENO1* gene (Semenza et al., 1996); and pRSV-LacZ, containing RSV promoter and β-galactosidase (β-gal) coding sequences. The ratio of luciferase to β-gal activity is a measure of HIF-1 transcriptional activity. Cells were transfected with plasmid DNA using Lipofectamine (Invitrogen, Carlsbad, CA) as described (Yuan et al., 2005). Briefly, cells were plated in 60 mm tissue culture plates at a density of 1×10^5 cells/plate in serum containing growth medium. After 24 h, the DNA–liposome mixture containing 1 μg of p2.1 and 0.25 μg of pRSV-LacZ with 10 μg of Lipofectamine in 2 ml of serum-free medium was added to cells and incubated for 4 h, followed by addition of 2 ml of complete (serum-containing) medium. After 24 h, cells were starved in serum-free growth medium for 18 h, and exposed to either 20% O_2 or IH. The Bright-Glo™ Luciferase Assay System (Promega, Madison, WI) was used to measure luciferase activity in cell lysates. Protein analysis was performed using a protein assay kit (Bio-Rad, Richmond, CA). We verified that all reporter gene assays were in the linear range. The protocols for transient transfection with HA3-HIF-1α plasmid were the same as with p2.1 plasmid.

Measurements of NOX and HIF-1α mRNA expression

Real-time reverse transcriptase (RT)-PCR was performed using a MiniOpticon system (Bio-Rad) with SYBR GreenER two-step qRT-PCR kit (Invitrogen) as previously described (Peng et al., 2009). Briefly, RNA was extracted from PC12 cells, mouse carotid bodies, cerebral cortex, and brain stem using TRIZOL and a 1 μg aliquot was reverse transcribed using Superscript III (Bio-Rad). Primer sequences for real-time RT-PCR amplification are shown in Table 1. Relative mRNA level (R) was calculated based on the comparative threshold (C_T) method using the formula $R = 2^{-\Delta CT}$, where ΔC_T is the difference between the threshold cycle of the given target mRNA in normoxia and IH. The C_T value was taken

as a fractional cycle number at which the emitted fluorescence of the sample passes a fixed threshold above the baseline and the values were normalized to an internal standard (18*S* rRNA). Purity and specificity of all products were confirmed by omitting the template and by performing a standard melting curve analysis.

Measurement of NADPH oxidase (Nox) activity

Membrane-enriched protein fractions from PC12 cells and various tissues were isolated (Li and Shah, 2002) and Nox activity was measured using a cytochrome c reduction assay (Li et al., 2001; Khan et al., 2010). Briefly, 100 μg aliquots of membrane proteins were incubated in 25 mM HEPES buffer (pH 7.0) with 150 μm cytochrome *c*, 100 μm NADPH for 30 min at 37°C in the presence and absence of superoxide dismutase (Sod; 200 U/ml). Cytochrome *c* reduction was measured by determining absorbance at 550 nm. The amount of SOD-inhibitable Nox activity expressed in nmol/min/mg protein was calculated using an extinction coefficient of 21 mM^{-1} cm^{-1}.

Studies with short interfering RNAs (siRNAs)

PC12 cells (5×10^5) were plated on collagen type IV (BD Biosciences, Bedford, MA) coated culture dishes and cultured for 24 h before transfection with siRNA (Santa Cruz) specific for HIF-1α, Nox2, or a scrambled (control) sequence at a concentration of 100 pmol/ml using DharmaFECT 2 (Dharmacon Research). Transfected cells were cultured in complete medium for 48 h before exposure to 60 cycles of IH or normoxia.

Data analysis

The data are expressed as mean ± SEM from 3 to 5 independent experiments each performed in triplicate. Statistical analysis was performed by analysis of variance (ANOVA) and *P*-values <0.05 were considered significant.

Results

IH increases Nox2 expression and activity in cultured PC12 cells

PC12 cells, which represent a cell culture model system for O_2-sensitive catecholamine-producing cells such as those in the carotid body and adrenal medulla (Yuan et al., 2005, 2008), were exposed to IH consisting of alternating cycles of hypoxia (1.5% O_2 for 30 sec) and re-oxygenation (20% O_2 for 5 min). Under these conditions, Nox2 mRNA (Fig. 1A), Nox2 protein (Fig. 1B), and Nox enzyme activity (Fig. 1C) increased progressively as the duration of IH was increased from 10 to 30 to 60 cycles. An siRNA-mediated loss-of-function approach was employed to ascertain the contribution of Nox2 to the IH-induced increase in Nox activity. Cells were transfected with Nox2 siRNA or control scrambled siRNA and then were exposed to 60 cycles of IH (IH_{60}) or normoxia. The IH_{60}-elicited increases in Nox2 protein expression and Nox enzyme activity were blocked in cells transfected with Nox2 siRNA but not in cells transfected with the scrambled siRNA (Fig. 1D,E). These results indicate that Nox2 is the major isoform responsible for the increased Nox activity that is induced by IH in PC12 cells. In the following experiments, we therefore investigated the molecular mechanisms underlying increased Nox2 expression in response to IH.

Pharmacological inhibition of HIF-1 blocks Nox2 expression in response to IH

To investigate whether HIF-1 is required for IH-induced Nox2 expression, a pharmacological approach was first employed. Digoxin and other cardiac glycosides have been shown to inhibit HIF-1α protein synthesis (Zhang et al., 2008b). We therefore examined the effects of digoxin on HIF-1 activation, Nox2 mRNA expression, and Nox enzyme activity in IH_{60}-exposed PC12 cells. IH_{60} increased HIF-1α accumulation and digoxin prevented this response in a concentration-dependent manner (Fig. 2A). To demonstrate the effects of digoxin on HIF-1 transcriptional activity, PC12 cells were transfected with reporter gene p2.1, in which the expression of firefly luciferase was driven by a HIF-1-dependent HRE upstream of an SV40 promoter (Semenza et al., 1996). We previously reported that in PC12 cells the induction of HRE-dependent transcriptional activity requires 120 cycles of IH (Yuan et al., 2005). As shown in Figure 2B, digoxin inhibited HIF-1-mediated transcriptional activation of the HIF-1 reporter gene in response to IH. Finally, digoxin, at the same concentration that blocked HIF-1 activation, significantly attenuated IH-induced Nox2 mRNA expression (Fig. 2C) and Nox enzyme activity (Fig. 2D).

To further demonstrate the validity of the pharmacological approach, we exposed PC12 cells to YC-1, a structurally distinct inhibitor of HIF-1 that induces the degradation of HIF-1α (Yeo et al., 2003). Like digoxin, YC-1 blocked IH-induced HIF-1α accumulation (Fig. 3A) and HIF-1 transcriptional activity (Fig. 3B). YC-1 also significantly attenuated the induction of Nox2 mRNA expression (Fig. 3C) and Nox enzyme activity (Fig. 3D).

Genetic ablation of HIF-1α blocks induction of Nox2 expression by IH

Expression of siRNA was employed to further establish a role for HIF-1 in Nox2 up-regulation by IH. PC12 cells were transfected with siRNA targeting HIF-1α and then exposed to IH_{60}. In cells transfected with HIF-1α siRNA, IH-induced increases in HIF-1α mRNA, HIF-1α protein, and HIF-1 transcriptional activity were absent (Fig. 4A–C). IH-evoked induction of Nox2 mRNA expression and enzyme activity were markedly reduced in cells transfected with HIF-1α siRNA but not in control cells treated with scrambled siRNA (Fig. 4D,E).

To determine whether the effects of IH are observed in other cell types, experiments were performed with HIF-1α-deficient (KO) mouse embryonic fibroblast (MEFs; Feldser et al., 1999). Basal HIF-1-dependent reporter activity was significantly less in KO MEFs compared to WT MEFs ($P < 0.01$; n = 5) and IH_{120} increased HIF-1-dependent transcriptional activity in WT, but not in KO, MEFs (Fig. 5A). Basal Nox2 mRNA expression was significantly less in KO compared to WT MEFs ($P < 0.01$; n = 5). WT MEFs, like PC12 cells, responded to IH with increased Nox2 mRNA, protein, and enzyme activity, and these responses were absent in KO MEFs (Fig. 5B–D). Thus, two different pharmacological inhibitors and two different genetic strategies for HIF-1α loss-of-function in two different cell types demonstrated that HIF-1 activation is required for induction of Nox2 expression and activity in response to IH.

Increased HIF-1α up-regulates Nox2 expression and activity

The effect of increasing HIF-1α expression (gain of function) was examined to further establish a link between HIF-1α and Nox2 expression and activity. To this end, PC12 cells were treated with either deferoxamine (DFO; 1 mM) an iron chelator for 20 h or transfected with a HIF-1α expression vector. The levels of HIF-1α protein and HRE activity were significantly increased in cells treated with DFO (Fig. 6A,B). Increased HIF-1 activation was associated with significant increases in Nox2 mRNA expression and Nox2 enzyme activity (Fig. 6C,D). Similar results were obtained in PC12 following overexpression of HIF-1α (Fig. 6E,H). Taken together, the studies in Figures 2–6 demonstrate that increased HIF-1α levels are necessary to increase Nox2 expression in cells subjected to IH and sufficient to increase Nox2 in cells transfected with HIF-1α expression vector.

Effects of IH on Nox2 expression in WT and *Hif1a*$^{+/-}$ mice

Previous studies demonstrated increased ROS in the cerebral cortex of IH-exposed WT, but not *Hif1a*$^{+/-}$ mice (Peng et al., 2006). We therefore exposed mice to IH for 10 days and analyzed Nox2 expression in various regions of the CNS and carotid bodies. IH increased Nox2 mRNA, Nox2 protein, Nox enzyme activity, and HIF-1α protein in cerebral cortex and brain stem, but not in cerebellum of WT mice (Fig. 7A–C). IH also increased Nox2 mRNA levels in carotid bodies (Fig. 7A). Nox2 protein and enzyme activity were not determined in carotid bodies because of limited quantities of tissue (wet weight, 25 μg). Intraperitoneal injection of digoxin (1 mg/kg/day) blocked the effects of IH on HIF-1α protein and Nox2 mRNA, protein, and enzyme activity in WT mice (Fig. 7A–C). In IH-exposed *Hif1a*$^{+/-}$ mice, increased accumulation of HIF-1α protein and up-regulation of Nox2 expression were not observed (Fig. 7A–C).

We previously reported that ROS-dependent phosphorylation and activation of PLCγ, PKC, and mTOR are critical for HIF-1α accumulation in PC12 cells exposed to IH (Yuan et al., 2008). As shown in Figure 8, IH increased phospho-PLCγ, phospho-PKC, and phospho-mTOR levels in cerebral cortex and brainstem, but not in cerebellum, from IH-exposed mice. These results are consistent with the lack of IH-induced HIF-1α protein and IH-induced Nox2 mRNA, protein, and enzyme activity in the cerebellum of IH-exposed mice (Fig. 7). Because of the presence of a feed-forward mechanism, it is not clear at what point the IH-induced ROS → PLCγ/PKC/mTOR → HIF-1 → NOX2 → ROS pathway is blocked in the cerebellum. Nevertheless, the coordinate induction (or not) of HIF-1α and Nox2 in different regions of the brain and in WT versus *Hif1a*$^{+/-}$ mice provide strong support for the critical role of HIF-1 in activating Nox2 expression in response to IH.

Discussion

We previously reported that (i) IH increases oxidant stress and HIF-1α expression in the carotid body and CNS and (ii) treatment with free radical scavengers blocks IH-induced HIF-1α expression, hypertension, and augmented ventilatory response to hypoxia. These results indicated that IH-induced ROS, leading to HIF-1 activation, is required for carotid body responses that result in alterations in cardiovascular and respiratory physiology, that is, HIF-1 acts downstream of ROS. We subsequently delineated the PLCγ/PKC/mTOR signal

transduction pathway by which IH-induced ROS lead to HIF-1 activation in PC12 cells (Yuan et al., 2005, 2008). However, we also found that IH increased oxidant stress in the cerebral cortex and induced hypertension in WT, but not *Hif1a*$^{+/-}$, mice (Peng et al., 2006), which indicated that HIF-1 acts upstream of ROS production. These findings suggested a feed-forward mechanism by which ROS induces HIF-1, leading to further increases in ROS production and downstream pathogenic sequelae. Nox2 mRNA, protein expression, and enzyme activity were induced by IH, both in PC12 cells (Yuan et al., 2008) and in carotid bodies of rodents, and *Nox2*$^{-/-}$ mice were deficient in carotid body responses to IH (Peng et al., 2009). In the present study, using genetic and pharmacological approaches to effect loss or gain of HIF-1α function, we demonstrate that HIF-1 mediates increased Nox2 expression in response to IH, thereby providing a molecular mechanism for the feed-forward relationship between ROS and HIF-1 in IH. Additional studies are required to determine whether HIF-1 binds directly to the *Nox2* gene and activates its transcription in response to IH.

Taken together, the results of the present study and previously published work (Peng et al., 2006) demonstrate that HIF-1α plays a pro-oxidant role in the setting of IH by increasing Nox activity. In contrast, HIF-2α plays an anti-oxidant role by mediating the expression of Sod2 and HIF-2α levels decline in response to IH (Nanduri et al., 2009). Thus, the combined effects of increased HIF-1α-dependent Nox2 expression and decreased HIF-2α-dependent Sod2 expression are responsible for the dramatic increase in ROS levels observed in response to IH. The pro-oxidant role of HIF-1 in the maladaptive (pathological) setting of IH is also in contrast to the anti-oxidant role of HIF-1 in the adaptive (physiological) response to continuous hypoxia, in which HIF-1 mediates the expression of multiple pathways that modulate or decrease mitochondrial respiration and ROS generation (Kim et al., 2006; Fukuda et al., 2007; Zhang et al., 2008a; Chan et al., 2009; Chen et al., 2010; Favaro et al., 2010).

In the present study, we also found that IH induces ROS and HIF-1α in the cerebral cortex and brain stem, but not in the cerebellum. Two important conclusions can be drawn from these data. First, in addition to the peripheral nervous system (i.e., carotid body), the HIF-1α → Nox2 → ROS pathway is likely to mediate responses to IH in the CNS as well. Second, activation of the HIF-1α → Nox2 → ROS pathway appears to be anatomically selective in the CNS. The lack of HIF-1 activation in cerebellum by IH is associated with the lack of phosphorylation of PLCγ, PKC, and mTOR (upstream activators of HIF-1) as well as the absence of Nox2 expression (downstream HIF-1 target gene). Delineating the molecular basis and functional consequences of tissue-specific HIF-1 activation and Nox2 expression in response to IH represent important goals for future research. Finally, just as HIF-1 activation in the CNS in addition to the carotid body may play a critical role in mediating autonomic morbidities associated with IH, other HIF-1 target genes in addition to *Nox2* may also be involved as downstream effectors. Further studies are needed to test the hypothesis that HIF-1 plays a central role not only in the initiation but also in the systems integration of autonomic responses to IH.

Acknowledgments

This work was supported by grants from National Institutes of Health, Heart, Lung and Blood Institute HL-90554, HL-76537, HL-86493, HL-089616 (to N.R.P.) and by funds from the Johns Hopkins Institute for Cell Engineering. G.L.S. is the C. Michael Armstrong Professor at The Johns Hopkins University School of Medicine.

Literature Cited

Bao G, Metreveli N, Li R, Taylor A, Fletcher EC. Blood pressure response to chronic episodic hypoxia: Role of the sympathetic nervous system. J Appl Physiol. 1997; 83:95–101. [PubMed: 9216950]

Bedard K, Krause KH. The NOX family of ROS-generating NADPH oxidases: Physiology and pathophysiology. Physiol Rev. 2007; 87:245–313. [PubMed: 17237347]

Chan SY, Zhang YY, Hemann C, Mahoney CE, Zweier JL, Loscalzo J. MicroRNA-210 controls mitochondrial metabolism during hypoxia by repressing the iron–sulfur cluster assembly proteins ISCU1/2. Cell Metab. 2009; 10:273–284. [PubMed: 19808020]

Chen Z, Li Y, Zhang H, Huang P, Luthra R. Hypoxia-regulated microRNA-210 modulates mitochondrial function and decreases ISCU and COX10 expression. Oncogene. 2010; 29:4362–4368. [PubMed: 20498629]

Del Rio R, Moya EA, Iturriaga R. Carotid body and cardiorespiratory alterations in intermittent hypoxia: The oxidative link. Eur Respir J. 2010; 36:143–150. [PubMed: 19996187]

Favaro E, Ramachandran A, McCormick R, Gee H, Blancher C, Crosby M, Devlin C, Blick C, Buffa F, Li JL, Vojnovic B, Pires das Neves R, Glazer P, Iborra F, Ivan M, Ragoussis J, Harris AL. MicroRNA-210 regulates mitochondrial free radical response to hypoxia and Krebs cycle in cancer cells by targeting iron sulfur cluster protein ISCU. PLoS ONE. 2010; 5:e10345. [PubMed: 20436681]

Feldser D, Agani F, Iyer NV, Pak B, Ferreira G, Semenza GL. Reciprocal positive regulation of hypoxia-inducible factor 1alpha and insulin-like growth factor 2. Cancer Res. 1999; 59:3915–3918. [PubMed: 10463582]

Fletcher EC, Lesske J, Qian W, Miller CC III, Unger T. Repetitive, episodic hypoxia causes diurnal elevation of blood pressure in rats. Hypertension. 1992; 19:555–561. [PubMed: 1592450]

Fukuda R, Zhang H, Kim JW, Shimoda L, Dang CV, Semenza GL. HIF-1 regulates cytochrome oxidase subunits to optimize efficiency of respiration in hypoxic cells. Cell. 2007; 129:111–122. [PubMed: 17418790]

Iyer NV, Kotch LE, Agani F, Leung SW, Laughner E, Wenger RH, Gassmann M, Gearhart JD, Lawler AM, Yu AY, Semenza GL. Cellular and developmental control of O_2 homeostasis by hypoxia-inducible factor 1a. Genes Dev. 1998; 12:149–162. [PubMed: 9436976]

Khan S, Nanduri J, Yuan G, Kinsman B, Kumar GK, Joseph J, Kalyanaraman B, Prabhakar NR. Nox2 mediates intermittent hypoxia-induced mitochondrial complex I inhibition: Relevance to blood pressure changes in rats. Antioxid Redox Signal. 2010; 14:533–542. [PubMed: 20618070]

Kim JW, Tchernyshyov I, Semenza GL, Dang CV. HIF-1-mediated expression of pyruvate dehydrogenase kinase: A metabolic switch required for cellular adaptation to hypoxia. Cell Metab. 2006; 3:177–185. [PubMed: 16517405]

Kumar GK, Rai V, Sharma SD, Ramakrishnan DP, Peng YJ, Souvannakitti D, Prabhakar NR. Chronic intermittent hypoxia induces hypoxia-evoked catecholamine efflux in adult rat adrenal medulla via oxidative stress. J Physiol. 2006; 575:229–239. [PubMed: 16777938]

Kuri BA, Khan SA, Chan SA, Prabhakar NR, Smith CB. Increased secretory capacity of mouse adrenal chromaffin cells by chronic intermittent hypoxia: Involvement of protein kinase C. J Physiol. 2007; 584:313–319. [PubMed: 17702812]

Li JM, Shah AM. Intracellular localization and preassembly of the NADPH oxidase complex in cultured endothelial cells. J Biol Chem. 2002; 277:19952–19960. [PubMed: 11893732]

Li JM, Mullen AM, Shah AM. Phenotypic properties and characteristics of superoxide production by mouse coronary microvascular endothelial cells. J Mol Cell Cardiol. 2001; 33:1119–1131. [PubMed: 11444917]

Mole DR, Blancher C, Copley RR, Pollard PJ, Gleadle JM, Ragoussis J, Ratcliffe PJ. Genome-wide association of hypoxia-inducible factor (HIF)-1a and HIF-2a DNA binding with expression profiling of hypoxia-inducible transcripts. J Biol Chem. 2009; 284:16767–16775. [PubMed: 19386601]

Nanduri J, Wang N, Yuan G, Khan SA, Souvannakitti D, Peng YJ, Kumar GK, Garcia JA, Prabhakar NR. Intermittent hypoxia degrades HIF-2a via calpains resulting in oxidative stress: Implications for recurrent apnea-induced morbidities. Proc Natl Acad Sci USA. 2009; 106:1199–1204. [PubMed: 19147445]

Narkiewicz K, Somers VK. The sympathetic nervous system and obstructive sleep apnea: Implications for hypertension. J Hypertens. 1997; 15:1613–1619. [PubMed: 9488212]

Nieto FJ, Young TB, Lind BK, Shahar E, Samet JM, Redline S, D'Agostino RB, Newman AB, Lebowitz MD, Pickering TG. Association of sleep-disordered breathing, sleep apnea, and hypertension in a large community-based study. Sleep Heart Health Study. JAMA. 2000; 283:1829–1836. [PubMed: 10770144]

Peng YJ, Prabhakar NR. Effect of two paradigms of chronic intermittent hypoxia on carotid body sensory activity. J Appl Physiol. 2004; 96:1236–1242. [PubMed: 14660510]

Peng YJ, Overholt JL, Kline D, Kumar GK, Prabhakar NR. Induction of sensory long-term facilitation in the carotid body by intermittent hypoxia: Implications for recurrent apneas. Proc Natl Acad Sci USA. 2003; 100:10073–10078. [PubMed: 12907705]

Peng YJ, Yuan G, Ramakrishnan D, Sharma SD, Bosch-Marce M, Kumar GK, Semenza GL, Prabhakar NR. Heterozygous HIF-1a deficiency impairs carotid body-mediated systemic responses and reactive oxygen species generation in mice exposed to intermittent hypoxia. J Physiol. 2006; 577:705–716. [PubMed: 16973705]

Peng YJ, Nanduri J, Yuan G, Wang N, Deneris E, Pendyala S, Natarajan V, Kumar GK, Prabhakar NR. NADPH oxidase is required for the sensory plasticity of the carotid body by chronic intermittent hypoxia. J Neurosci. 2009; 29:4903–4910. [PubMed: 19369559]

Peppard PE, Young T, Palta M, Skatrud J. Prospective study of the association between sleep-disordered breathing and hypertension. N Engl J Med. 2000; 342:1378–1384. [PubMed: 10805822]

Poets CF, Samuels MP, Southall DP. Epidemiology and pathophysiology of apnoea of prematurity. Biol Neonate. 1994; 65:211–219. [PubMed: 8038285]

Prabhakar NR, Kumar GK. Mechanisms of sympathetic activation and blood pressure elevation by intermittent hypoxia. Respir Physiol Neurobiol. 2010; 174:156–161. [PubMed: 20804865]

Semenza GL. Regulation of oxygen homeostasis by hypoxia-inducible factor 1. Physiology (Bethesda). 2009; 24:97–106. [PubMed: 19364912]

Semenza GL, Jiang BH, Leung SW, Passantino R, Concordet JP, Maire P, Giallongo A. Hypoxia response elements in the aldolase A, enolase 1, and lactate dehydrogenase A gene promoters contain essential binding sites for hypoxia-inducible factor 1. J Biol Chem. 1996; 271:32529–32537. [PubMed: 8955077]

Souvannakitti D, Kumar GK, Fox A, Prabhakar NR. Neonatal intermittent hypoxia leads to long-lasting facilitation of acute hypoxia-evoked catecholamine secretion from rat chromaffin cells. J Neurophysiol. 2009; 101:2837–2846. [PubMed: 19339466]

Souvannakitti D, Nanduri J, Yuan G, Kumar GK, Fox AP, Prabhakar NR. NADPH oxidase-dependent regulation of T-type Ca^{2+} channels and ryanodine receptors mediate the augmented exocytosis of catecholamines from intermittent hypoxia-treated neonatal rat chromaffin cells. J Neurosci. 2010; 30:10763–10772. [PubMed: 20705601]

Troncoso Brindeiro CM, da Silva AQ, Allahdadi KJ, Youngblood V, Kanagy NL. Reactive oxygen species contribute to sleep apnea-induced hypertension in rats. Am J Physiol Heart Circ Physiol. 2007; 293:H2971–H2976. [PubMed: 17766485]

Wang GL, Jiang BH, Rue EA, Semenza GL. Hypoxia-inducible factor 1 is a basic-helix-loop-helix-PAS heterodimer regulated by cellular O_2 tension. Proc Natl Acad Sci USA. 1995; 92:5510–5514. [PubMed: 7539918]

Yeo EJ, Chun YS, Cho YS, Kim J, Lee JC, Kim MS, Park JW. YC-1: A potential anticancer drug targeting hypoxia-inducible factor 1. J Natl Cancer Inst. 2003; 95:516–525. [PubMed: 12671019]

Yuan G, Nanduri J, Bhasker CR, Semenza GL, Prabhakar NR. Ca^{2+}/calmodulin kinase-dependent activation of hypoxia inducible factor 1 transcriptional activity in cells subjected to intermittent hypoxia. J Biol Chem. 2005; 280:4321–4328. [PubMed: 15569687]

Yuan G, Nanduri J, Khan S, Semenza GL, Prabhakar NR. Induction of HIF-1a expression by intermittent hypoxia: involvement of NADPH oxidase, Ca^{2+} signaling, prolyl hydroxylases, and mTOR. J Cell Physiol. 2008; 217:674–685. [PubMed: 18651560]

Zhan G, Serrano F, Fenik P, Hsu R, Kong L, Pratico D, Klann E, Veasey SC. NADPH oxidase mediates hypersomnolence and brain oxidative injury in a murine model of sleep apnea. Am J Respir Crit Care Med. 2005; 172:921–929. [PubMed: 15994465]

Zhang H, Bosch-Marce M, Shimoda LA, Tan YS, Baek JH, Wesley JB, Gonzalez FJ, Semenza GL. Mitochondrial autophagy is an HIF-1-dependent adaptive metabolic response to hypoxia. J Biol Chem. 2008a; 283:10892–10903. [PubMed: 18281291]

Zhang H, Qian DZ, Tan YS, Lee K, Gao P, Ren YR, Rey S, Hammers H, Chang D, Pili R, Dang CV, Liu JO, Semenza GL. Digoxin and other cardiac glycosides inhibit HIF-1a synthesis and block tumor growth. Proc Natl Acad Sci USA. 2008b; 105:19579–19586. [PubMed: 19020076]

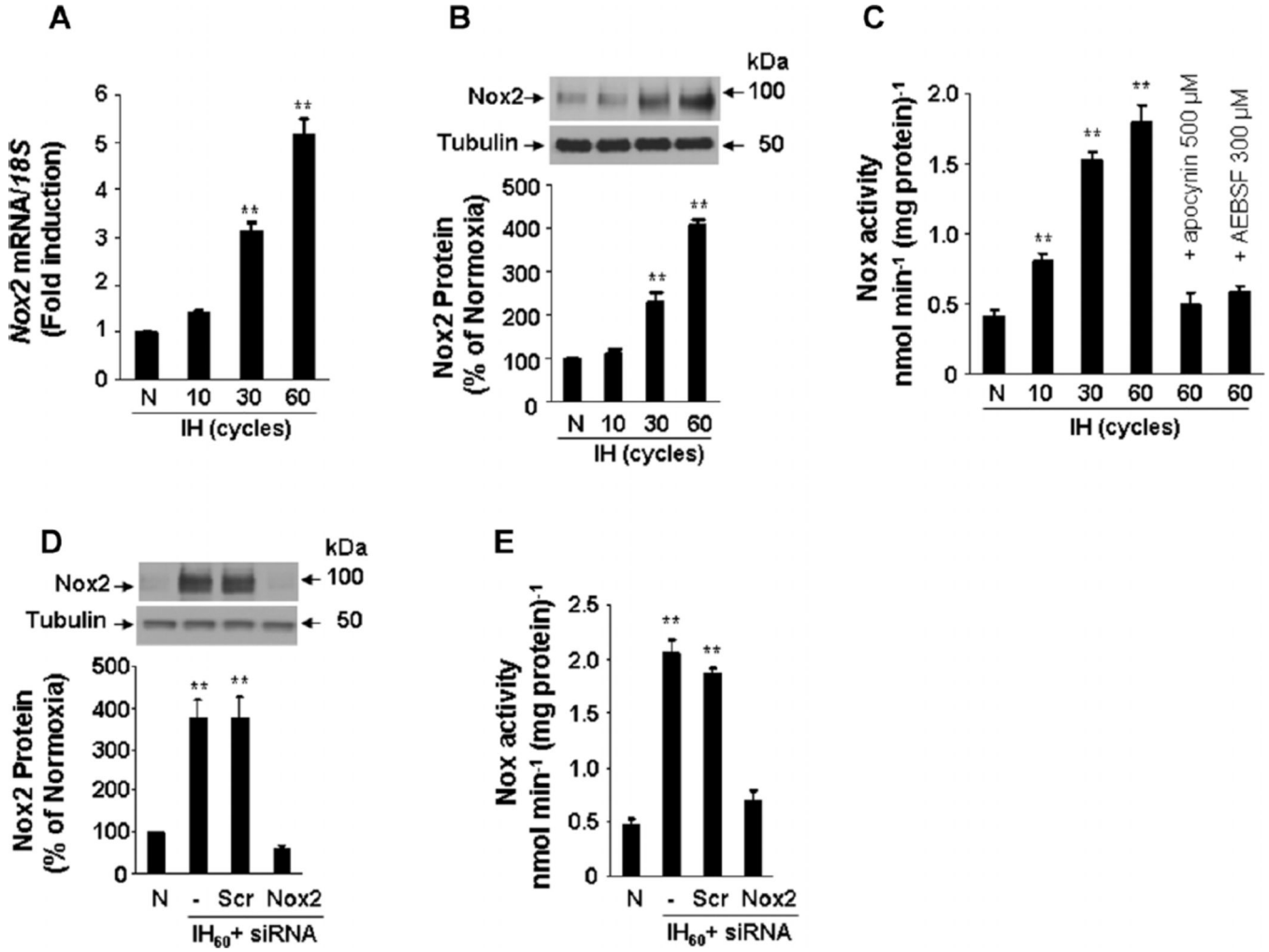

Fig. 1.

Nox2 up-regulation by IH in PC12 cells. A: Analysis of Nox2 mRNA expression. Cells were exposed to 20% O_2 (N) or to 10–60 cycles of IH (30 sec at 1.5% O_2 alternated with 5 min at 20% O_2). Real-time reverse-transcription PCR assay was performed to determine the ratio of Nox2 mRNA to 18*S* rRNA. The results were normalized to those obtained from normoxic cells. B: Nox2 protein expression. Western blot assay was performed on lysates from cells exposed to 0–60 cycles of IH. *Top part*, representative Nox2 immunoblot. *Bottom part*, densitometric analysis of Nox2 protein normalized to tubulin expression and expressed as percent change from normoxic control (N).C: Analysis of Nox enzyme activity. Nox activity was analyzed in membrane fractions from cells exposed to 0–60 cycles of IH as described in Materials and Methods. Apocynin (500 µM) and AEBSF (300 µM), inhibitors of Nox, added to cells before IH exposure prevented increased Nox activity in IH_{60}-exposed cells. D: Nox2 siRNA prevents IH_{60}-induced up-regulation of Nox2 protein. Cells were transfected with either Nox2 or scrambled siRNA and then exposed to IH_{60}. *Top part*, representative Nox2 and tubulin (control protein) immunoblot assays. *Bottom part*, densitometric analysis of Nox2 protein normalized to tubulin expression and expressed as percent of normoxic control (N).E: Analysis of Nox enzyme activity in siRNA-transfected

PC12 cells exposed to IH_{60}. Mean ± SEM (n = 3–5) are shown, $^{**}P < 0.01$ compared with control (N).

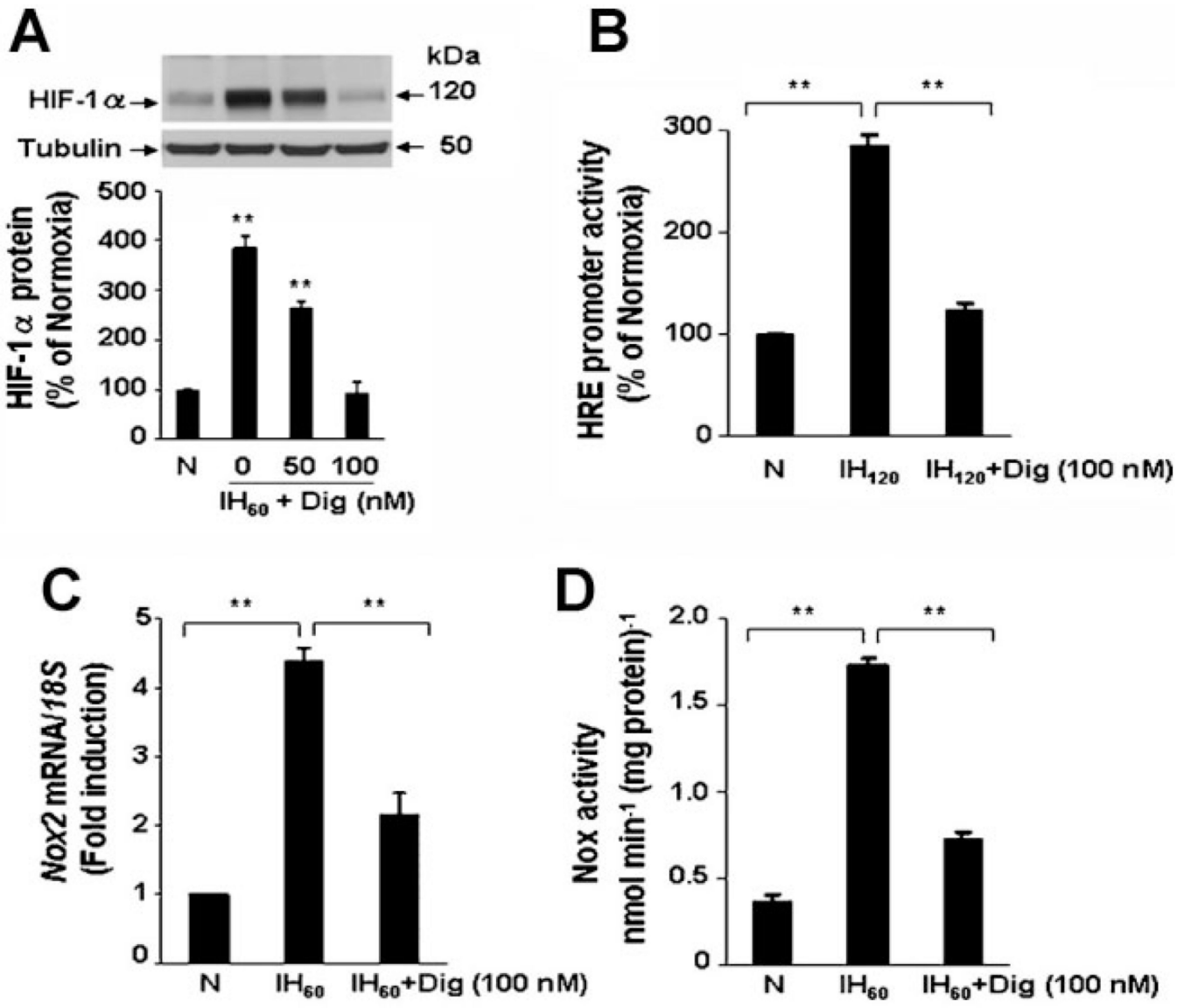

Fig. 2.

Digoxin blocks HIF-1 activation and Nox2 up-regulation by IH. A: Digoxin inhibits IH_{60}-evoked HIF-1α accumulation in a concentration-dependent manner. *Top part*, representative HIF-1α immunoblot. *Bottom part*, densitometric analysis of HIF-1α protein levels normalized to tubulin protein levels and expressed as percent change from normoxic control (N). B: Digoxin inhibits HIF-1-dependent reporter gene expression by IH. PC12 cells were cotransfected with p2.1, containing an HRE upstream of SV40 promoter and luciferase coding sequences, and pRSV-LacZ, containing RSV promoter and β-gal coding sequences. Transfected cells were exposed to either 20% O_2 (N) or 120 cycles of IH (IH 120). C,D: Digoxin inhibits up-regulation of Nox2 mRNA expression (C) and Nox enzyme activity (D) in response to IH. Mean ± SEM (n = 3–5) are shown, $^{**}P < 0.01$ compared with control (N).

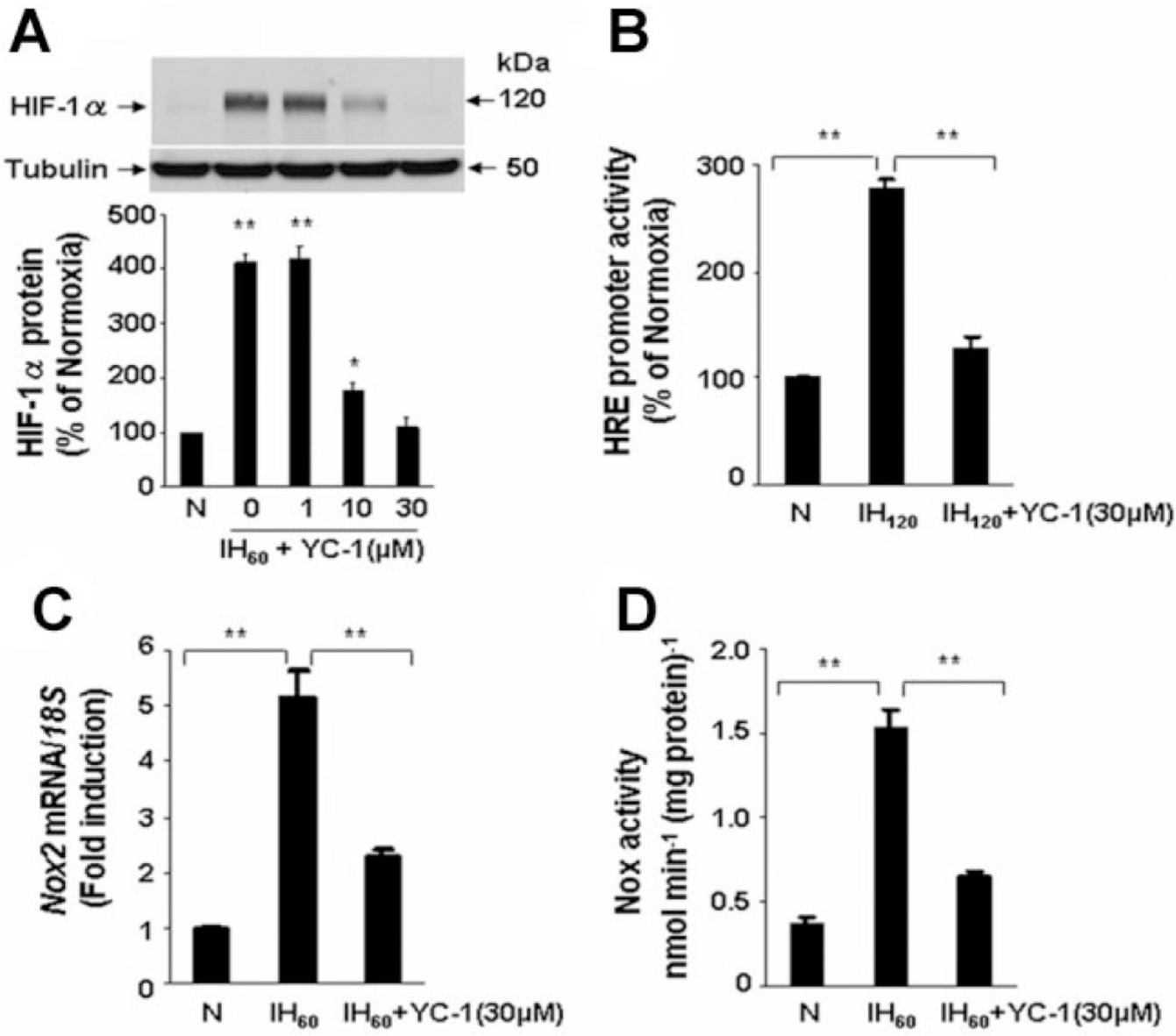

Fig. 3.

YC-1 inhibits HIF-1 activation and Nox2 up-regulation in PC12 cells exposed to IH. A: YC-1 blocks IH_{60}-evoked HIF-1α accumulation in a concentration-dependent manner. *Top part*, representative HIF-1α immunoblot. *Bottom part*, densitometric analysis of HIF-1α protein levels normalized to tubulin levels and expressed as percent change from normoxic control (N). B: YC-1 inhibits HIF-1-dependent reporter gene expression in response to IH. C,D: YC-1 blocks up-regulation of Nox2 mRNA expression (C) and Nox enzyme activity (D) by IH. Mean ± SEM (n = 3–5) are shown, $^{**}P < 0.01$ compared with control (N).

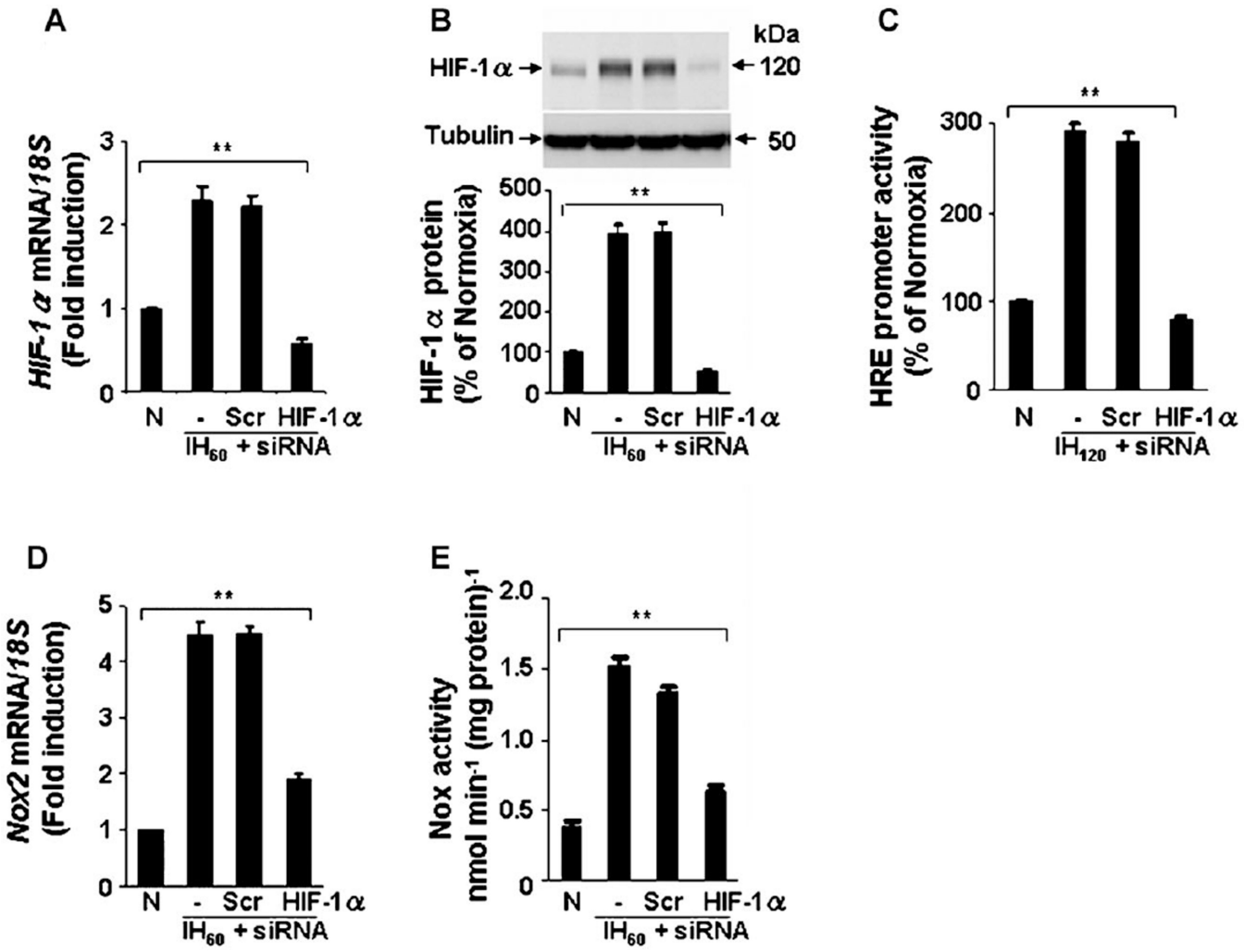

Fig. 4.

Silencing of HIF-1α by siRNA abolishes Nox2 up-regulation in IH-exposed cells. A–C: Absence of HIF-1α mRNA up-regulation (A), protein accumulation (B), and HRE reporter gene expression (C) in IH-exposed PC12 cells transfected with HIF-1α siRNA. Cells were transfected with either HIF-1α or control scrambled (Scr) siRNA and then were exposed to IH. *Upper parts* in B, representative examples of HIF-1α and tubulin immunoblots. *Lower parts* in B, densitometric analysis of HIF-1α protein normalized to tubulin expression and presented as percent of normoxic control, respectively. D,E: IH_{60}-induced up-regulation of Nox2 mRNA expression (D) and Nox2 activity (E) were significantly attenuated in cells transfected with HIF-1α, but not with Scr, siRNA. Mean ± SEM (n = 5) are shown. $^{**}P < 0.01$ compared with control (N).

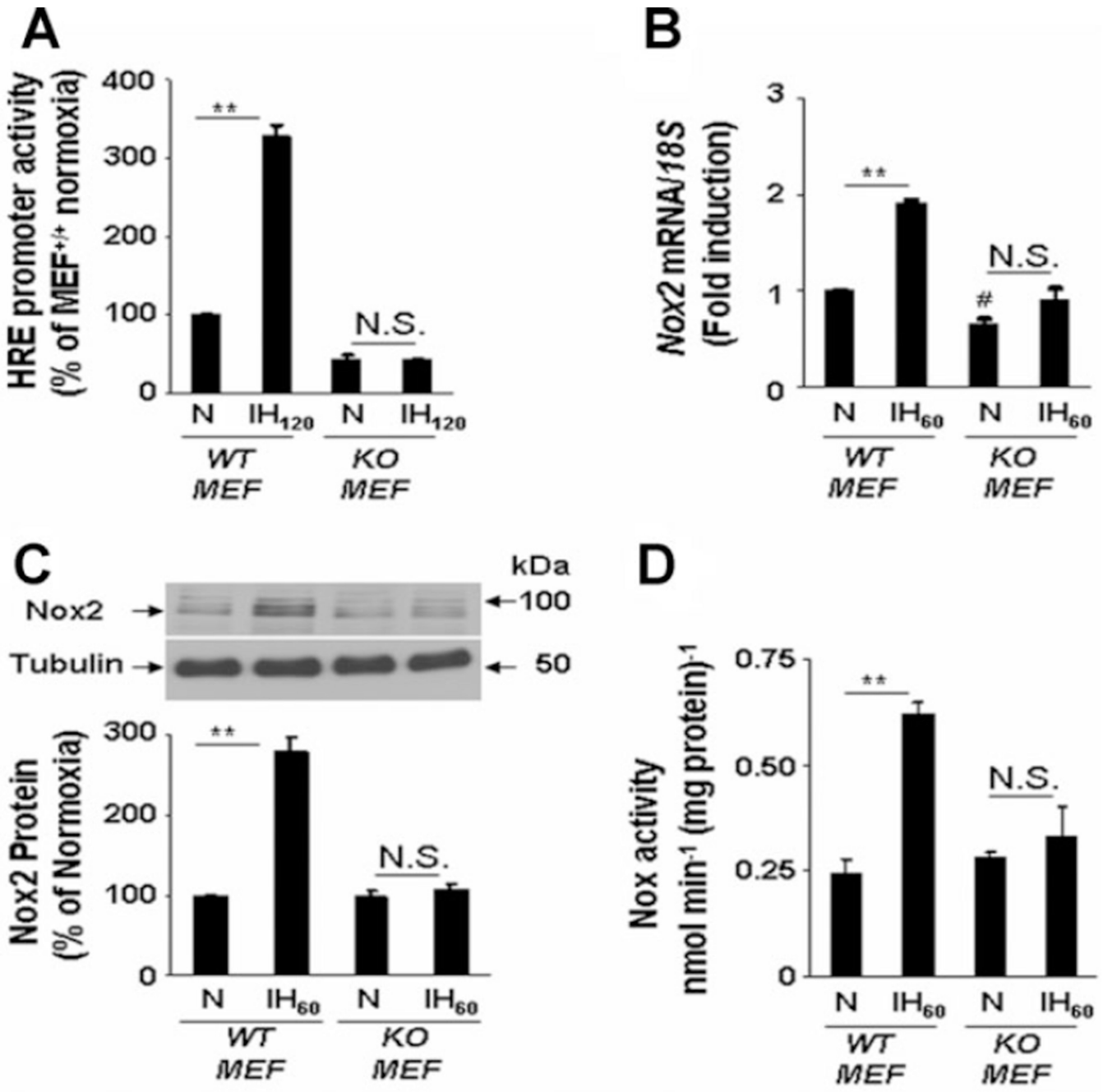

Fig. 5.

Absence of Nox2 activation in HIF-1α-deficient mouse embryonic fibroblasts (MEFs) exposed to IH. A: Activation of HRE reporter gene expression by IH_{120} in wild-type (WT) MEFs and absence of this response in HIF-1α knockout (KO) MEFs. B–D: Absence of IH_{60}-induced up-regulation of Nox2 mRNA (B) and protein (C) expression and enzyme activity (D) in KO MEFs. Mean ± SEM (n = 5) are shown. $^{**}P < 0.01$; $^{\#}P < 0.05$; and N.S., not significant ($P > 0.05$) compared with normoxic controls (N).

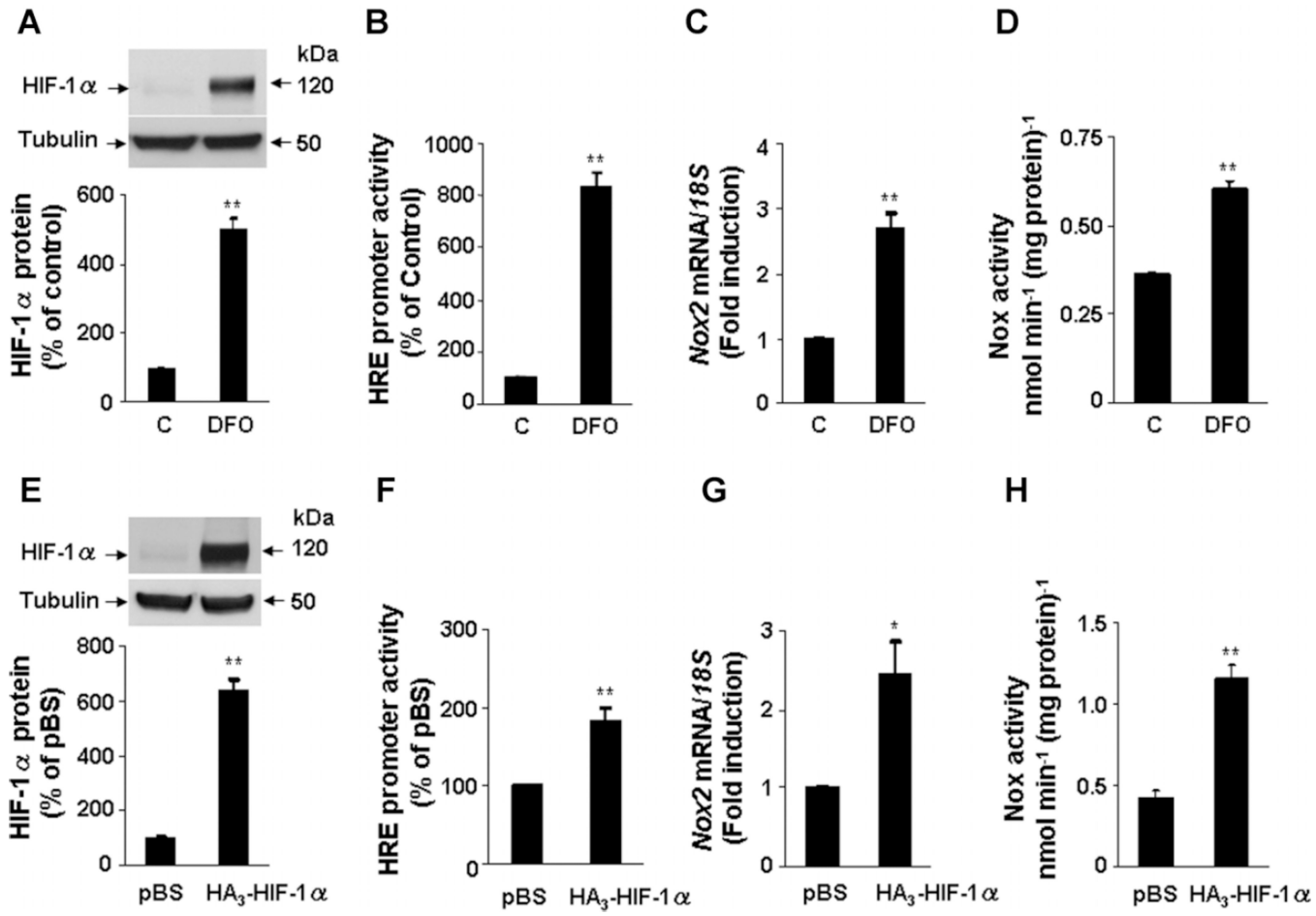

Fig. 6.

HIF-1α overexpression increases Nox2 expression and activity. A: Deferoxamine (1 mM; DFO) treatment for 20 h increases HIF-1α accumulation in PC12 cells. *Top part*, representative HIF-1α immunoblot. *Bottom part*, densitometric analysis of HIF-1α protein levels normalized to tubulin levels and expressed as percent change from control (C). B–D: DFO increases HIF-1-dependent gene expression (B) Nox2 mRNA expression (C) and Nox enzyme activity (D). E: PC12 cells were transfected with 1 μg of either basic vector (pBS) or HIF-1α plasmid (HA_3-HIF-1α). *Top part*, representative HIF-1α immunoblot. *Bottom part*, densitometric analysis of HIF-1α protein levels normalized to tubulin levels. F–H: Overexpression of HIF-1α increases HIF-1-dependent gene expression (F), Nox2 mRNA expression (G), and Nox enzyme activity (H). Mean ± SEM (n = 4) are shown; $^{**}P < 0.01$ compared with control (C) or pBS.

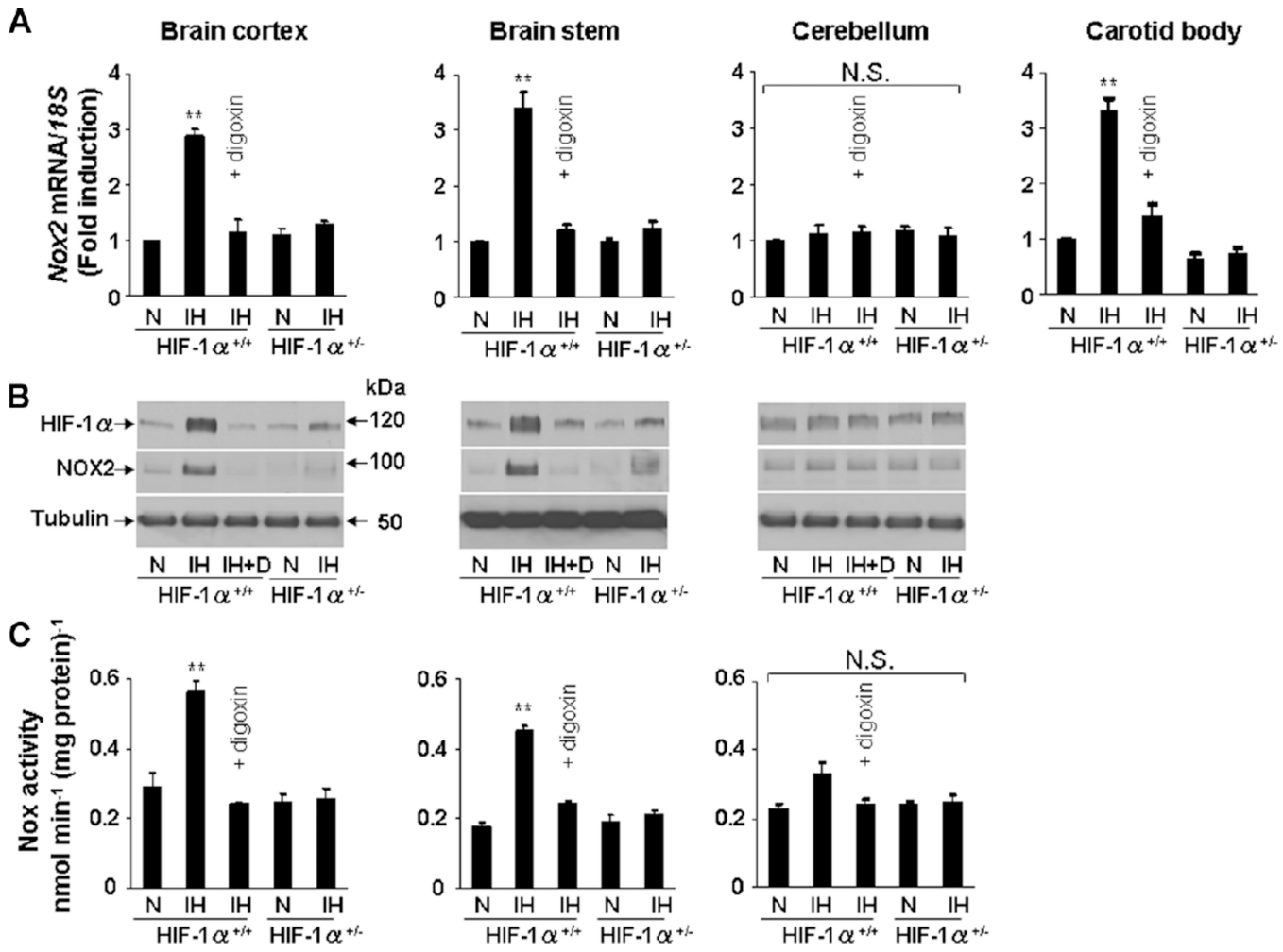

Fig. 7.

Effect of IH on Nox2 expression in the central nervous system and carotid bodies in *Hif1*α$^{+/+}$ wild-type (WT) and *Hif1*α$^{+/-}$ heterozygous-knockout mice. A–C: Age and sex-matched WT mice were exposed to normoxia (N) or IH (8 h/day × 10 days) and concurrently treated with vehicle (IH) ordigoxin (IH + D;1 mg/kg/day IP) and littermate *Hif1*α$^{+/-}$ mice were exposed to Nor IH. Nox2 mRNA (A), HIF-1α and Nox2 proteins (B), and Nox enzyme activity (C) were analyzed in brain cortex, brain stem, and cerebellum. Nox2 mRNA levels in the carotid body were determined in the same mice (A). Mean ± SEM (n = 5 mice in each group) are shown. ***P* < 0.01 and N.S., not significant (*P* > 0.05) compared with normoxic controls (N).

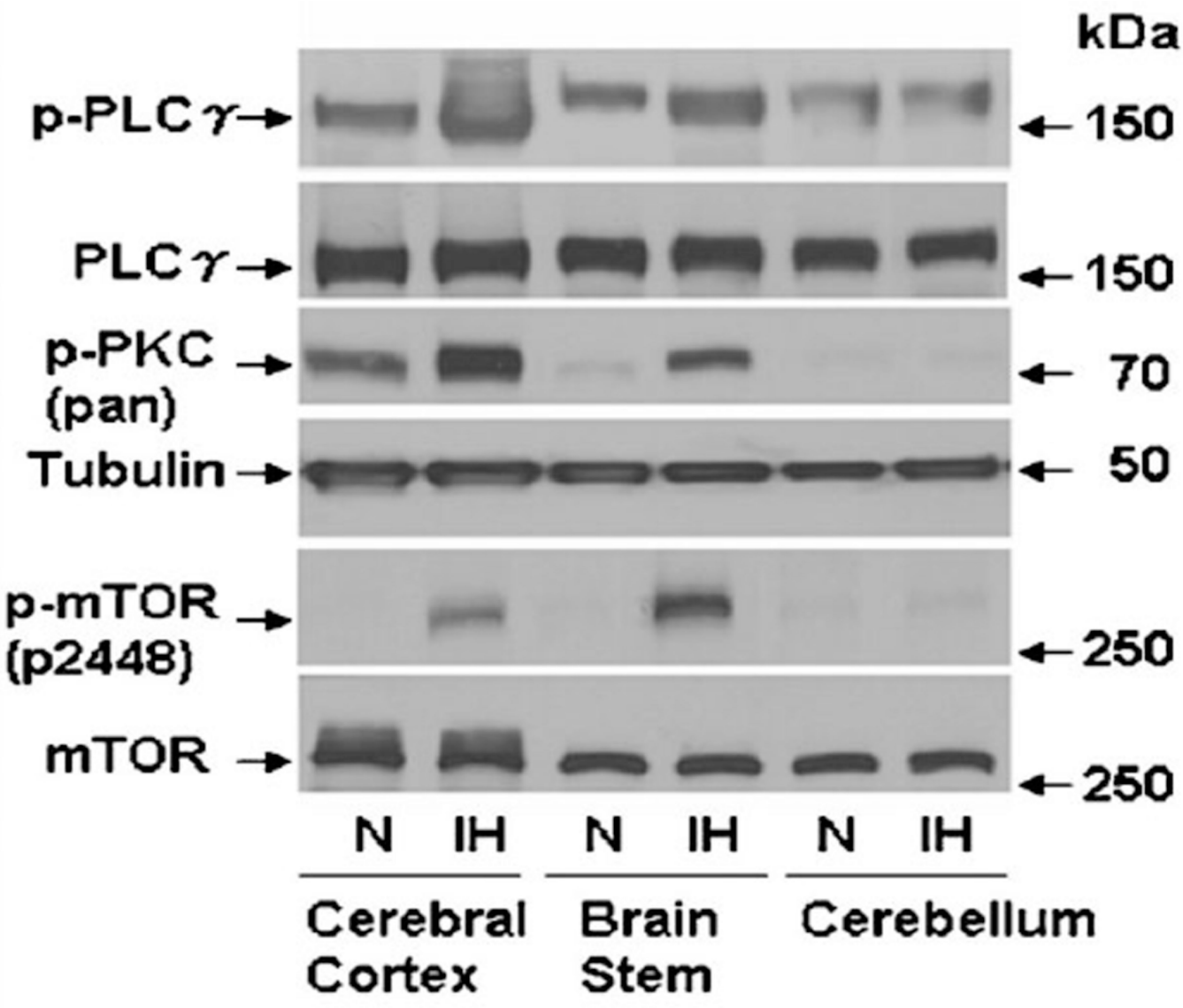

Fig. 8.

Effect of IH on phosphorylated PLCγ, PKC, and mTOR levels in the brain cortex, brain stem, and cerebellum of mice. Adult male BALB/c mice were exposed to normoxia (N) or IH (8 h/day × 10 days). Levels of phospho-PLCγ (p-PLCγ), total PLCγ (PLCγ), phospho-PKC (p-PKC), total PKC (PKC), phosphorylated mTOR (p-mTOR), and total mTOR (mTOR) were determined by immunoblot assays of tissue lysates prepared from cerebral cortex, brain stem, and cerebellum.

TABLE 1

Primers for quantitative real-time RT-PCR assays

Name	Nucleotide sequence	Size	GeneBank #
rNox2-FWD	GTGGAGTGGTGTGAATG	219	NM_023965
rNox2-REV	TTTGGTGGAGGATGTGATGA		
rHIF-1α-FWD	CCACAGGACAGTACAGGAG	150	NM_024359
rHIF-1α-REV	TCAAGTCGTGCTGAATAATC		
r18S-FWD	GTAACCCGTTGAACCCCATT	151	X01117
r18S-REV	CCATCCAATCGGTAGTAGCG		
mNox2-FWD	AGCTATGAGGTGGTGATGTTAGTGG	88	NM_007807
mNox2-REV	CACAATATTTGTACCAGACAGACTTGAG		